Biomedicine & Pharmacotherapy 140 (2021) 111679

Contents lists available at ScienceDirect

Biomedicine & Pharmacotherapy

journal homepage: www.elsevier.com/locate/biopha

Comparative study on beneficial effects of vitamins B and D in attenuating doxorubicin induced cardiotoxicity in rats: Emphasis on calcium homeostasis

Heba H. Awad [a], Marwa O. El-Derany [b], Eman M. Mantawy [c], Haidy E. Michel [c], Mona M. El-Naa [d], Rania A. Salah El-Din [e], Amany I. El-Brairy [a], Ebtehal El-Demerdash [c,*]

[a] Department of Pharmacology & Toxicology, Faculty of Pharmacy, October University for Modern Sciences & Arts (MSA University), Cairo, Egypt
[b] Department of Biochemistry, Faculty of Pharmacy, Ain Shams University, Cairo, Egypt
[c] Department of Pharmacology & Toxicology, Faculty of Pharmacy, Ain Shams University, Cairo, Egypt
[d] Department of Pharmacology & Toxicology, Faculty of Pharmacy, University of Sadat City, Sadat City, Egypt
[e] Department of Anatomy, Faculty of Medicine, Ain Shams University, Cairo, Egypt

ARTICLE INFO

Keywords:
Doxorubicin
Cardiotoxicity
Calcium
Nicotinamide
Vitamin D
Alfacalcidol

ABSTRACT

The use of doxorubicin (DOX) to treat various tumors is limited by its cardiotoxicity. This study aimed to investigate and compare the cardioprotective effects of nicotinamide (NAM) and alfacalcidol (1α(OH)D_3), against DOX-induced cardiotoxicity. Sprague Dawley male rats received DOX (5 mg/kg, i.p.) once/week for four consecutive weeks. Treated groups received either NAM (600 mg/kg, p.o.) for 28 consecutive days or 1α(OH)D_3 (0.5 ug/kg, i.p.) once/week for four consecutive weeks. DOX elicited marked cardiac tissue injury manifested by elevated serum cardiotoxicity indices, conduction and histopathological abnormalities. Both NAM and 1α(OH)D_3 successfully reversed all these changes. From the mechanistic point of view, DOX provoked intense cytosolic and mitochondrial calcium (Ca^{2+}) overload hence switching on calpain1 (CPN1) and mitochondrial-mediated apoptotic cascades as confirmed by upregulating Bax and caspase-3 while downregulating Bcl-2 expression. DOX also disrupted cardiac bioenergetics as evidenced by adenosine triphosphate (ATP) depletion and a declined ATP/ADP ratio. Moreover, DOX upregulated the Ca^{2+} sensor; calmodulin kinase II gamma (CaMKII-δ) which further contributed to cardiac damage. Interestingly, co-treatment with either NAM or 1α(OH)D_3 reversed all DOX associated abnormalities by preserving Ca^{2+} homeostasis, replenishing ATP stores and obstructing apoptotic events. Additionally, DOX prompted nuclear factor kappa B (NF-κB) dependent inflammatory responses and subsequently upregulated interleukin-6 (IL-6) expression. Co-treatment with NAM or 1α(OH)D_3 effectively obstructed these inflammatory signals. Remarkably, NAM showed superior beneficial cardioprotective properties over 1α(OH)D_3. Both NAM and 1α(OH)D_3 efficiently attenuated DOX-cardiomyopathy mainly via preserving Ca^{2+} homeostasis and diminishing apoptotic and inflammatory pathways. NAM definitely exhibited effective cardioprotective capabilities over 1α(OH)D_3.

1. Introduction

Doxorubicin (DOX), an anthracycline antibiotic, is considered the mainstay in the treatment of a wide variety of human malignancies such as breast, lung and ovarian cancers [1]. notwithstanding its potent antitumor effect, the use of DOX has been obstructed by several deleterious and fatal adverse effects hindering its clinical use [2]. Cardiotoxicity is considered the most significant and frequent toxicity

Abbreviations: ACASP-3, activated caspase-3; ATP, Adinosine triphosphate; ADP, Adinosine diphosphate; 1αOHD3, alfacalcidol; BW, Body Weight; Ca^{2+}, Calcium; CPN-1, Calpain-1; CaMKIIδ, Calcium calmodulin Kinase II δ; CTn1, Cardiac Triponin-1; CK-MB, Creatine kinase isoenzyme-MB; DOX, Doxorubicin; ECG, Electrocardiography; ELISA, Enzyme-linked immunosorbent assay; EM, Electron Microscope; HW, Heart Weight; IL-6, interleukin-6; LDH, Lactate dehydrogenase; i.p., intraperitoneal; NAD^+, nicotinamide adenine dinucleotide; NAM, Nicotinamide; NFκB, Nuclear Factor Kappa B; PBS, phosphate buffer saline; RyR2, Ryanodine receptor; SERCA2a, Sarcoplasmic/ endoplasmic reticulum Ca(2+)ATPase 2a; SR, Sarcoplasmic Reticulum.

* Correspondence to: Pharmacology & Toxicology Department, Faculty of Pharmacy, Ain Shams University, Cairo 11566, Egypt.
E-mail address: ebtehal_dm@pharma.asu.edu.eg (E. El-Demerdash).

https://doi.org/10.1016/j.biopha.2021.111679
Received 22 February 2021; Received in revised form 25 April 2021; Accepted 27 April 2021
Available online 21 May 2021

associated with DOX [3]. A multitude of mechanisms have been implicated in the pathogenesis of DOX-induced cardiotoxicity. One of the profound mechanisms associated with DOX cardiotoxicity is linked to Ca^{2+} homeostasis dysregulation in cardiac tissue [4]. DOX down-regulates the expression of sarcoplasmic/endoplasmic reticulum Ca^{2+} ATPase2a (SERCA2a), a Ca^{2+} pump responsible for Ca^{2+} influx from cytosol to sarcoplasmic reticulum. Consequently, DOX elevates both cytosolic and mitochondrial Ca^{2+} levels [5]. This cytosolic Ca^{2+} level elevation is responsible for Ca^{2+}/calmodulin-dependent protein kinase II-gamma (CaMKIIδ) activation which contributes considerably towards the pathogenesis of DOX cardiotoxicity [6]. Activated CaMKIIδ promotes apoptosis through the calcium-dependent, non-lysosomal cysteine proteases enzyme calpain1 (CPN1) [7]. Moreover, whenever a certain threshold of mitochondrial Ca^{2+} level is reached, the opening of a mitochondrial permeability transition pore is triggered, allowing the release of cytochrome-C into the cytosol and hence formation of apoptosome, which in turn activates caspase-9 and ultimately result in apoptotic cell death [8]. DOX also prompts inflammatory responses via activation of the transcription of the nuclear factor kappa B (NF-κB) and consequent release of pro-inflammatory cytokines in the myocardium [9].

Recently, a diversity of natural compounds were investigated for their potential competences in mitigating DOX-induced cardiotoxicity [10]. Vitamins are among the biologically efficient compounds that have been reported extensively to alleviate cardiovascular disorders [11]. Nicotinamide (NAM) is the amide form of vitamin B_3 [12]. Vitamin B_3 have two common functional co-factors which are nicotinamide adenine dinucleotide (NAD+), nicotinamide adenine dinucleotide phosphate (NADP+) and their reduced forms (NAD(P)H). These cofactors, referred to as the NAD (P)(H) pool, are intimately involved in all essential bioenergetics, anabolic and catabolic pathways [13]. This pool also has crucial roles in cell metabolism and cell signaling through multiple pathways regulating intracellular Ca^{2+} signaling, mitochondrial respiration and ATP production. Manipulation of NAD+ bioavailability through vitamin B_3 supplementation has become a valuable nutritional and therapeutic avenue [14].

Vitamin D ($1,25(OH)_2D_3$) is a multifunctional micronutrient that is vital for human health [15]. Growing evidence suggests that low serum $1,25(OH)_2D_3$ levels are associated with high risk of cardiovascular disease such as hypertension, coronary artery disease, ischemic heart disease and strokes [16]. Indeed, endogenous $1,25(OH)_2D_3$ is important in inhibiting inflammatory pathways and modulating proinflammatory cytokines production protecting tissues from hyperinflammatory response damage [17,18]. Furthermore, $1,25(OH)_2D_3$ is a potent anti-oxidant facilitating the balance of mitochondrial activities and preventing oxidative stress-related protein oxidation, lipid peroxidation, and DNA damage [15]. Previous studies reported that hypovitaminosis D is associated with an elevation of intracellular Ca^{2+} and acceleration in cellular damage, apoptosis, and aging [15].

Vitamins as nutraceuticals offer a safe and bright prospect for future treatment and the prevention of cardiovascular toxicities and diseases. Accordingly, the aim of this study was to compare the potential protective effects of NAM and $1\alpha(OH)D_3$ in DOX-induced chronic cardiotoxicity through the elucidation of intracellular Ca^{2+} signaling that can greatly modulate inflammation, and the apoptotic status of the cardiomyocytes.

2. Material and methods

2.1. Material

Doxorubicin (DOX) was purchased as Adriablastine (50 mg DOX hydrochloride, Pharmacia and Upjohn, Milan, Italy). NAM was purchased from Sigma Chemical Co. (St.Louis, MO, USA). Vitamin D was purchased as One Alpha IV injection (alfacalcidol) from LEO Pharma (Hurley, Berkshire, UK). Formaldehyde 37% and phosphate buffered glutaraldehyde were purchased from El-Nasr Chemical Co. (Egypt). All other chemicals were of the highest commercially available grade of purity.

2.2. Animals

Adult Sprague Dawley male rats weighing between 150 and 220 gm (age: 10–12 weeks) were obtained from Nile Co. for Pharmaceutical and Chemical industries (Cairo, Egypt). The animals were acclimatized for two weeks before experimentation in an air-conditioned atmosphere at a temperature of 25 °C with alternating 12-hour light and dark cycles and allowed free access to standard diet pellets and water. The experimental protocol was conducted according to the ethical guidelines and was approved by the Research Ethics Committee of the Faculty of Pharmacy, Ain Shams University, Egypt under the Memorandum No. 54.

2.3. Experimental design

Based on our preliminary study (supplementary), the optimal cardioprotective dose of NAM was 600 mg/kg and $1\alpha(OH)D_3$ (0.5 ug/kg). The duration of the experiment was 28 days. Sixty adult male Sprague Dawley rats (150–220 g) were weighed and assigned randomly into six groups (10 rats per group). **The control group:** received distilled water through an oral gavage daily for 28 days. **The DOX group:** was given a single intraperitoneal (i.p.) injection of DOX (5 mg/kg) once a week for four consecutive weeks [19]. **The NAM + DOX group:** received an oral dose of NAM (600 mg/kg) daily for 28 days and DOX (once weekly, 5 mg/kg). **The $1\alpha(OH)D_3$ + DOX group:** received i.p. injection of $1\alpha(OH)D_3$ (0.5 ug/kg) [20] once weekly 48 h before the DOX injection (once weekly of 5 mg/kg) for four consecutive weeks. **The NAM group:** received NAM at an oral dose of 600 mg/kg daily for four consecutive weeks. **The $1\alpha(OH)D_3$ group:** received $1\alpha(OH)D_3$ (0.5 ug/kg) i.p. once weekly for four consecutive weeks (Fig. 1).

Forty-eight hours after the last DOX injection, the animals were weighed, anesthetized with ketamine (75 mg/kg; i.p.) and then subjected to ECG recording (Fig. 1). Blood samples were withdrawn from the retro-orbital plexus and allowed to clot. The blood samples were then centrifuged, and the serum was collected for biochemical analysis. Heart weights (HW) were recorded. Heart tissues were collected and homogenized in phosphate buffer saline (PBS). The homogenate was subsequently used for biochemical analysis. Some heart specimens were fixated in 10% buffered formalin for histopathological and immunohistochemical examination and other heart specimens were fixated immediately in 2.5% phosphate buffered glutaraldehyde (pH 7.4) for electron microscopic (EM) examination.

2.4. Electrocardiography (ECG)

The rats were anesthetized with ketamine (75 mg/kg; i.p.) and an electrocardiography (ECG) was recorded for 1 min. Heart rate, P duration, QRS Interval and QTc, were monitored using ECG Power Lab module which consists of Power-Lab/8sp and Animal Bio-Amplifier, Australia, in addition to Lab Chart7 software with ECG analyzer.

2.5. Determination of body and heart weights

The initial and final body weight (BW) of the rats and their HW were recorded for all study groups and their heart indices were calculated using the formula (HW / BW) ×100.

2.6. Assessment of serum cardiotoxicity indices

Serum creatine kinase isoenzyme-MB (CK-MB) and serum lactate dehydrogenase (LDH) activities were determined spectrophotometrically following the standard procedures using commercial kits obtained from Spectrum diagnostics, Cairo, Egypt. The serum level of cardiac

Fig (1)

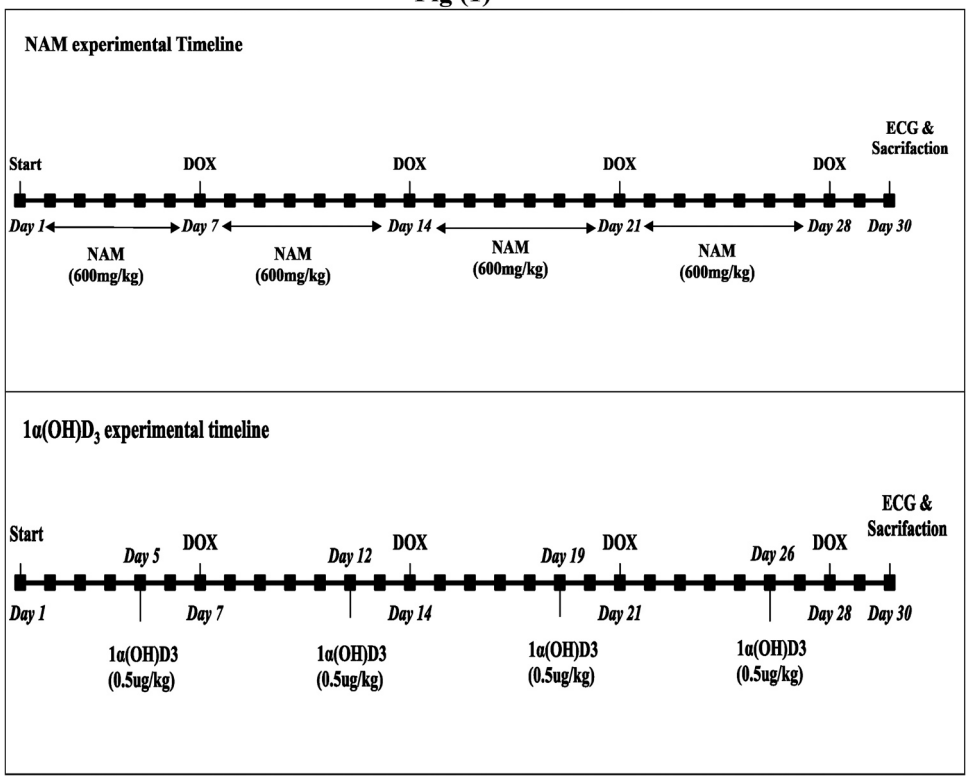

Fig. 1. Timeline of experimental study design and drug administration.

troponin I (c-TnI) was determined using enzyme-linked immunosorbent assay (ELISA) kit according to the manufacturer's instructions developed by Life Diagnostics Inc.

2.7. Histopathological and electron microscopic examination

Heart samples were processed for light and electron microscopy. For light microscopy, heart specimens were prepared and stained with hematoxylin and eosin (H and E) They were fixated in 10% formalin for 24 h and then washed with tap water, before using serial dilutions of alcohol for dehydration. Specimens were cleared in xylene and embedded in paraffin at 56ºC in hot water oven for 24 h. Paraffin bees wax tissue blocks were prepared for sectioning at 4 μm thickness by the slide microtome. Heart specimens were immediately fixated in 2.5% phosphate buffered glutaraldehyde (pH 7.4) at 4 7¯C for 24 h and post fixed in 1% osmium tetraoxide for 1 h, then dehydrated in ascending grades of ethanol for electron microscopic examination [21].

2.8. Assessment of cell viability markers

Heart tissues were homogenized in ice-cold PBS (0.02 mol/L, pH 7.0–7.2). The resulting homogenates were centrifuged for 15 min at 5000 rpm. The supernatant was separated, and assay was carried out following the standard procedures using the competitive inhibition enzyme immunoassay technique according to the manufacturer's instructions developed by My BioSource, Inc. for assessing both ATP and ADP content.

2.9. Assessment of cytoplasmic and mitochondrial calcium (Ca^{2+})

The mitochondria were isolated using the differential centrifugation method [22]. Heart specimen homogenate was centrifuged for 10 min at 600 rpm. The supernatant was centrifuged at 15,000 rpm for 5 min. The supernatant was the cytosolic fraction. The mitochondrial fraction was obtained from the pellet, after washing it with a buffer (containing sucrose 0.25 M, Tris-HCl 5 mM, potassium dihydrogen phosphate 3 mM and magnesium chloride 5 mM) and centrifuging it at 15,000 rpm for 5 min. The last step was repeated twice to ensure pure mitochondrial fraction. The spectrophotometric technique was used to determine the measurements of both cytosolic and mitochondrial Ca^{2+} levels [23]. Briefly, 25 μL of sample was incubated at room temperature with 500 μL of color reagent and 500 μL 2-amino-2-methylpropanol buffer for 15 min and then measured at 540 nm.

2.10. Assessment of calcium calmodulin kinase II gamma (CaMKIIδ)

The concentration of CaMKII-δ was assessed in the tissue homogenates using ELISA kits according to the manufacturer's instructions developed by Cloud-Clone Corp. USA.

2.11. Assessment of calpain1 (CPN1)

The calpain1 (CPN1) concentration was assessed in the tissue homogenates using ELISA kits according to the manufacturer's instructions (Bioassay Technology, China).

2.12. Assessment of apoptotic markers

Immunohistochemical staining was performed according to the manufacturer's protocol as previously described. Deparaffinized tissue sections were incubated with one of the following primary antibodies: mouse monoclonal BAX primary antibody (Thermo Fisher Scientific, Cat.#MA5-14003), rabbit polyclonal primary antibody Bcl-2 (Thermo Fisher Scientific, Cat.#PA1-30411), rabbit polyclonal primary antibody caspase-3 (Thermo Fisher Scientific, Cat.#RB-1197-R7). Quantitative measurement of activated caspase-3 (ACASP-3) in tissue homogenate was assessed using ELISA kits according to manufacturer's instructions developed by Cloud-Clone Corp. USA (SEA396Mu).

2.13. Assessment of inflammatory markers

ELISA was used for assessing the concentration of the inflammatory marker IL-6 in tissue homogenates according to the manufacturer's instructions (Bioassay Technology,China). Quantitative determination of nuclear NF-κB concentration was performed according to the manufacturer's protocol (Elabscience Biotechnology, Cat.#E-EL-R0917). Meanwhile immunohistochemistry was performed to determine of NF-κB expression in cardiac tissues. Immunohistochemical staining was performed according to the manufacturer's protocol. Deparaffinized tissue sections were incubated with the primary antibody: rabbit polyclonal NF-κB antibody (Thermo Fisher Scientific, Cat. #RB-1638-P0).

For all immunohistochemical staining of BAX, Bcl-2, caspase-3 and NF-κB, four non-overlapping fields (magnification, ×400) were randomly selected per tissue section of each sample to determine the positive immune-expression percentage levels. Morphological measurements and analyzed data were obtained using the Leica application module for tissue sections analysis attached to a Full HD microscope imaging system (Leica Microsystems GmbH, Germany). Image quantitation was performed using image software (version 1.48) to calculate the area percent (A%).

2.14. Statistical analysis

Data were presented as mean ± S.D. Statistical analysis was performed using one-way analysis variance (ANOVA) followed by Tukey-Kramer Post Hoc Test. The 0.05 level of probability was used as the criterion for significance. All statistical analyses were performed using Instat software package (version 8.4.2). Graphs were sketched using GraphPad prism software version 8 (ISI® software, USA).

3. Results

3.1. Effect of NAM or 1α(OH)D_3 on abnormal ECG

DOX intoxication provoked a significant bradycardia, and prolonged QRS complex, PR interval and QTc interval durations, compared with the control group. In contrast, compared with the DOX intoxicated group, co-administration of either NAM or 1α(OH)D_3 effectively reversed all the DOX-induced ECG abnormalities as evidenced by elevating the heart rate and decreasing the duration of both the QRS complex, PR interval and QTc interval (Fig. 2). However, no significant differences were detected between NAM or 1α(OH)D_3 + DOX intoxicated groups.

3.2. Effect of NAM or 1α(OH)D_3 on the final body weights and cardiac weight indices

DOX-treated rats showed a significant reduction in final BW by 18% and a significant increase in cardiac weight and cardiac index by 19% and 46%, respectively compared with the control group. On the other hand, NAM co-treatment of intoxicated rats significantly increased their BW by 11.93% and reduced both their cardiac weight and index by 13% and 22%, respectively compared with the DOX group. Rats co-treated with 1α(OH)D_3 and DOX showed a significant increase in BW by 6.89% and a significant decrease in cardiac weight and index by 12% and 19%, respectively compared with the DOX group. In comparison to 1α(OH)D_3 co-treatment, the NAM administration showed a significant reduction in cardiac index by 5% (Table 1).

3.3. Effect of NAM or 1α(OH)D_3 on the serum cardiotoxicity indices

As markers for myocardial injury, the activities of CK-MB and LDH enzymes and expression of c-TnI were assessed in serum. Serum CK-MB, LDH and c-TnI were significantly elevated in the DOX group by 31%, 12% and 25%, respectively, when compared with the control group. NAM co-treatment showed a significant reduction in serum CK-MB, LDH and c-TnI levels by 16%, 11% and 14%, respectively, compared with the DOX group. Meanwhile, 1α(OH)D_3 co-treatment induced significant reduction in the activities of serum CK-MB, LDH and c-TnI levels by 10%, 6% and 13%, respectively, when compared with the DOX group (Table 2). No significant difference in CK-MB, LDH or c-TnI was detected between the DOX-intoxicated rats co-treated with either NAM or 1α(OH)D_3.

3.4. Effect of NAM or 1α(OH)D_3 on histopathological and electron microscope alterations

Heart tissues from the control group showed a normal appearance and arrangement of cardiac muscle fibers (Fig. 3A). On the contrary, DOX intoxication prompted prominent histopathological changes in cardiac tissues in the form of a disarrangement and degeneration of the myocardial muscle and widespread vacuolization, focal pyknosis in the myocardium associated with congestion in the myocardial blood vessels (Fig. 3B). Interestingly, cotreatment with either NAM or 1α(OH)D_3 along with DOX efficiently improved these histopathological abnormalities. Indeed, NAM co-treatment exerted more obvious cytoprotective effects on the myocardial cells as shown by intact cardiomyocytes and minimal degenerated and fragmented muscle cells (Fig. 3C) while 1α(OH)D_3 co-treatment still showed wide areas of degenerative changes of cardiomyocytes with intercellular spaces (Fig. 3D). Treatment with either NAM or 1α(OH)D_3 alone showed no alterations in the normal cardiac myocyte architecture (Fig. 3E and F).

Upon EM examination, the transmission electron micrographs of the control group showed linear muscle fiber composed of several cardiac muscle cells joined end to end at specialized junctional zones. Each cell had an elongated nucleus centrally located in the sarcoplasm that bound by a sarcolemma. The mitochondria were uniform in size. The myofibrils are formed of regular sarcomeres with distinct Z lines (Fig. 4A). Meanwhile, the DOX treated group showed disorganized cardiomyocytes with irregular shaped nuclei characterized by an aggregation of nuclear chromatin and dissociation of the outer nuclear membrane and perinuclear edema. The mitochondria showed significant disarrangement and non-uniform size. The variation in mitochondrial size is due to the continuous replacement of damaged mitochondria by newly synthesized ones to sustain the constant need for ATPs. The non-uniform sized electron dense mitochondria of were characterized by enlarged size, loss of inter-mitochondrial contacts, mitochondrial cavitation, swelling and fragmentation. In addition, the DOX-treated group showed areas of myofibril lysis, disordered arrangement and loss of Z- and M- bands together with a loss of normal sarcomere appearance. Interestingly, some vessels showed damage to the endothelial lining (Fig. 4B and C). Meanwhile, the NAM+DOX group showed myofibrils formed of regular sarcomeres with minimal areas of myofibril lysis and mitochondria of a nearly uniform size (Fig. 4D). On the other hand, the 1α(OH)D_3 +DOX treated group showed arranged cardiac muscle fibers and cells joined end to end at specialized junctional zones. However, the mitochondria were not uniform in size and arranged irregularly and each cell had an elongated nucleus centrally located in the sarcoplasm (Fig. 4E). Interestingly, the EM examination of the myocardium after administration of NAM showed better reservation of mitochondrial integrity and size compared with 1α(OH)D_3. Finally, the muscle fiber in both NAM and 1α(OH)D_3 groups showed normal architecture features of cardiac cells (Fig. 4F and G).

3.5. Effect of NAM or 1α(OH)D_3 on cardiomyocytes viability markers

In the DOX group, the ATP/ADP ratio was significantly decreased by 76%, as compared with the control group. When compared with the DOX group, the NAM+DOX treated group presented a significant increase in ATP/ADP ratio by 319%. Meanwhile, rats treated with 1α(OH)D_3 + DOX exhibited significant elevation ATP/ADP ratio by 230% as

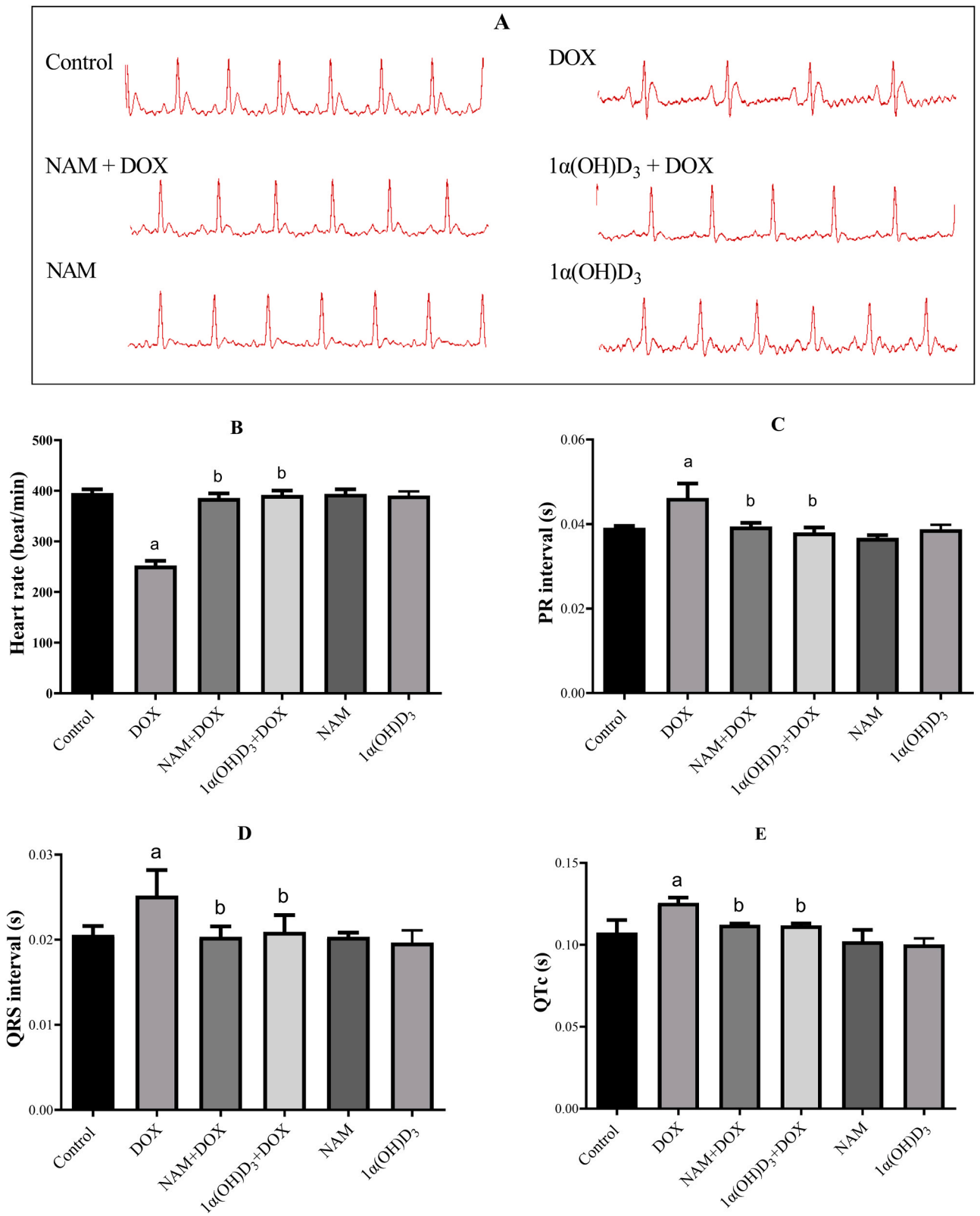

Fig. 2. Effect of NAM or $1\alpha(OH)D_3$ on ECG abnormalities in DOX-induced cardiotoxicity. (A) ECG graph, (B) Heart rate (beat/min), (C) PR interval (s), (D) QRS duration (s) (E) QTc interval (s). Data are represented as mean ± SD (n = 8–10). a,b,c: statistically significant from control, DOX or NAM + DOX, respectively at $P < 0.05$ using one-way ANOVA followed by Tukey-Kramer Post Hoc test.

Table 1
Effect of NAM or 1α(OH)D_3 on body weight, heart weight,cardiac index and survival%.

Treated groups	Body Weight (gm)		Heart Weight (gm)	Cardiac index x10^3	Survival%
	Initial	Final			
Control	212.5 ± 7.09	251.1 ± 6.46	0.57 ± 0.02	2.20	100
DOX	217.7 ± 5.61	206.1 ± 9.75[a]	0.67 ± 0.018[a]	3.26[a]	80
NAM + DOX	216.0 ± 5.46	230.7 ± 6.79[a,b]	0.59 ± 0.004[a,b]	2.57[a,b]	100
1α(OH)D_3+ DOX	215.8 ± 7.86	220.3 ± 6.22[a,b]	0.59 ± 0.009[a,b]	2.67[a,b,c]	100
NAM	214.7 ± 6.32	247.0 ± 7.76	0.56 ± 0.02	2.28	100
1α(OH)D_3	213.7 ± 7.90	250.9 ± 9.33	0.56 ± 0.023	2.22	100

Data are represented as mean ± SD (n = 8–10). a, b and c: Statistically significant from the control, DOX or NAM + DOX group, respectively at $P < 0.05$ using one-way ANOVA followed by Tukey-Kramer Post Hoc test.

Table 2
Effect of NAM or 1α(OH)D_3 on serum CK-MB, LDH and cardiac Troponin I (cTnI).

Treated groups	CK-MB (U/l)	LDH (U/l)	cTnI (ng/ml)
Control	31.63 ± 1.85	50.37 ± 1.45	3.62 ± 0.103
DOX	41.37 ± 1.46[a]	56.55 ± 1.38[a]	4.54 ± 0.163[a]
NAM + DOX	34.73 ± 1.89[b]	51.72 ± 1.35[b]	3.89 ± 0.103[a,b]
1α(OH)D_3 + DOX	33.55 ± 2.14[b]	52.90 ± 2.53[b]	3.97 ± 0.154[a,b]
NAM	32.83 ± 1.08	50.35 ± 1.38	3.67 ± 0.114
1α(OH)D_3	31.85 ± 1.12	50.37 ± 1.88	3.68 ± 0.111

Data are represented as mean ± SD (n = 8–10). a or b: Statistically significant from the control or DOX group, respectively at $P < 0.05$ using one-way ANOVA followed by Tukey-Kramer Post Hoc test.

compared with the DOX group. Interestingly, NAM + DOX treated group presented a significant increase in the ATP/ADP ratio by 27% as compared with the 1α(OH)D_3 + DOX (Fig. 5C).

3.6. Effect of NAM or 1α(OH)D_3 on cytosolic and mitochondrial Ca^{2+} levels

The cytosolic Ca^{2+} level in DOX treated rats increased significantly by 37% compared with the control group. Meanwhile, co-treatment with either NAM or 1α(OH)D_3 significantly decreased cytosolic Ca^{2+} levels by 26% and 19%, respectively, as compared with the DOX treated group. Interestingly, NAM + DOX treated group significantly decreased the cytosolic Ca^{2+} level by 8% compared to 1α(OH)D_3 + DOX group. (Fig. 6A). Similar results were obtained concerning the mitochondrial Ca^{2+} level which DOX significantly increased by 447% as compared with the control group. Co-treatment with both NAM and 1α(OH)D_3 perfectly attenuated the imbalance of mitochondrial Ca^{2+} overload caused by DOX. NAM and 1α(OH)D_3 significantly decreased the mitochondrial Ca^{2+} level by 80% and 76%, respectively as compared with the DOX treated group. NAM co-treatment was more effective in preserving the mitochondrial Ca^{2+} load where it demonstrated more significant reduction in the mitochondrial Ca^{2+} level by 18% as compared with the 1α(OH)D_3 + DOX group (Fig. 6B).

3.7. Effect of NAM or 1α(OH)D_3 on calmodulin Kinase II gamma (CaMKIIδ) content

There was a significant increase in CaMKII-δ by 30% in DOX-intoxicated rats as compared with the control group. On the other hand, NAM + DOX and 1α(OH)D_3 + DOX treated groups showed significant reduction in CaMKII-δ levels by 18% and 12%, respectively, compared with the DOX group. NAM+DOX-treated rats showed a more significant reduction by 7% over 1α(OH)D_3 + DOX-treated animals (Fig. 7A).

3.8. Effect of NAM or 1α(OH)D_3 on calpain 1 (CPN1)

There was a significant increase in the CPN1 content induced by DOX by 206% as compared with the control group. On the other hand, NAM co-treatment showed a significant decline in the CPN1 content by 45% as compared with the DOX-treated group. In parallel, co-treatment with 1α(OH)D_3 with DOX significantly reduced the CPN1 content by 38% as compared with the DOX group. Remarkably, there was a significant reduction in the NAM+DOX treated group by 12% as compared with 1α(OH)D_3 + DOX -treated rats (Fig. 7B).

3.9. Effect of NAM or 1α(OH)D_3 on apoptotic markers expression in myocardial tissues

Apoptotic changes induced by DOX were assessed by an immunohistochemical examination of Bax, Bcl-2 and caspase-3 proteins and the quantitative analysis of ACASP-3 (Figs. 8 and 9). DOX decreased the anti-apoptotic Bcl-2 and increased the pro-apoptotic Bax as compared with the control group. The semiquantitative analysis of the immunostaining showed a significant elevation in Bax: Bcl-2 ratio in DOX-treated rats compared with the control group. Moreover, each of the NAM and 1α(OH)D_3 co-administration ameliorated the DOX intoxication by increasing expression of Bcl-2 and decreasing BAX expression (Fig. 8B and C). In parallel a reduction in Bax: Bcl-2 ratio as compared with the DOX treated group was observed in both vitamins-cotreated groups (Fig. 8D).

The apoptotic effects of DOX were further confirmed by assessing caspase-3 expression where DOX extensively elevated the enzyme expression as shown by the intense immunostaining as compared with the control group. On the other hand, both NAM and 1α(OH)D_3 cotreatment markedly reduced caspase-3 expression as evidenced by minimal immunostaining (Fig. 9G). Upon comparison, there was no significant change between NAM or 1α(OH)D_3 co-treated groups in Bax, Bcl-2 and caspase-3 expression.

The apoptotic effect of DOX was further supported by a 121% increase in ACASP-3 levels as compared with the control group. When compared with the DOX-treated group, NAM co-treated animals showed a 17% significant decline in ACASP-3 content. Meanwhile, 1α(OH)D_3 co-treated group showed a significant reduction in ACASP-3 by 8% as compared with the DOX group. Remarkably, there was a significant reduction in the NAM+DOX-treated group by 10% as compared with 1α(OH)D_3 + DOX-treated rats (Fig. 9H).

3.10. Effect of NAM or 1α(OH)D_3 on inflammatory markers in myocardial tissues

The pro-inflammatory responses induced by DOX were manifested by assessment of the inflammatory markers; NF-κB and IL-6. Immunohistochemical examination of NF-κB expression revealed apparent upregulation in the expression of the inflammatory mediator following DOX intoxication as shown by the intense brown staining (Fig. 10B and G). On the contrary, co-treatment with either NAM or 1α(OH)D_3 intensely downregulated NF-kB expression as shown by the faint brown staining (Fig. 10C, D and G). In parallel, the nuclear content of NF-κB showed a significant rise by 143% in DOX group as compared with the

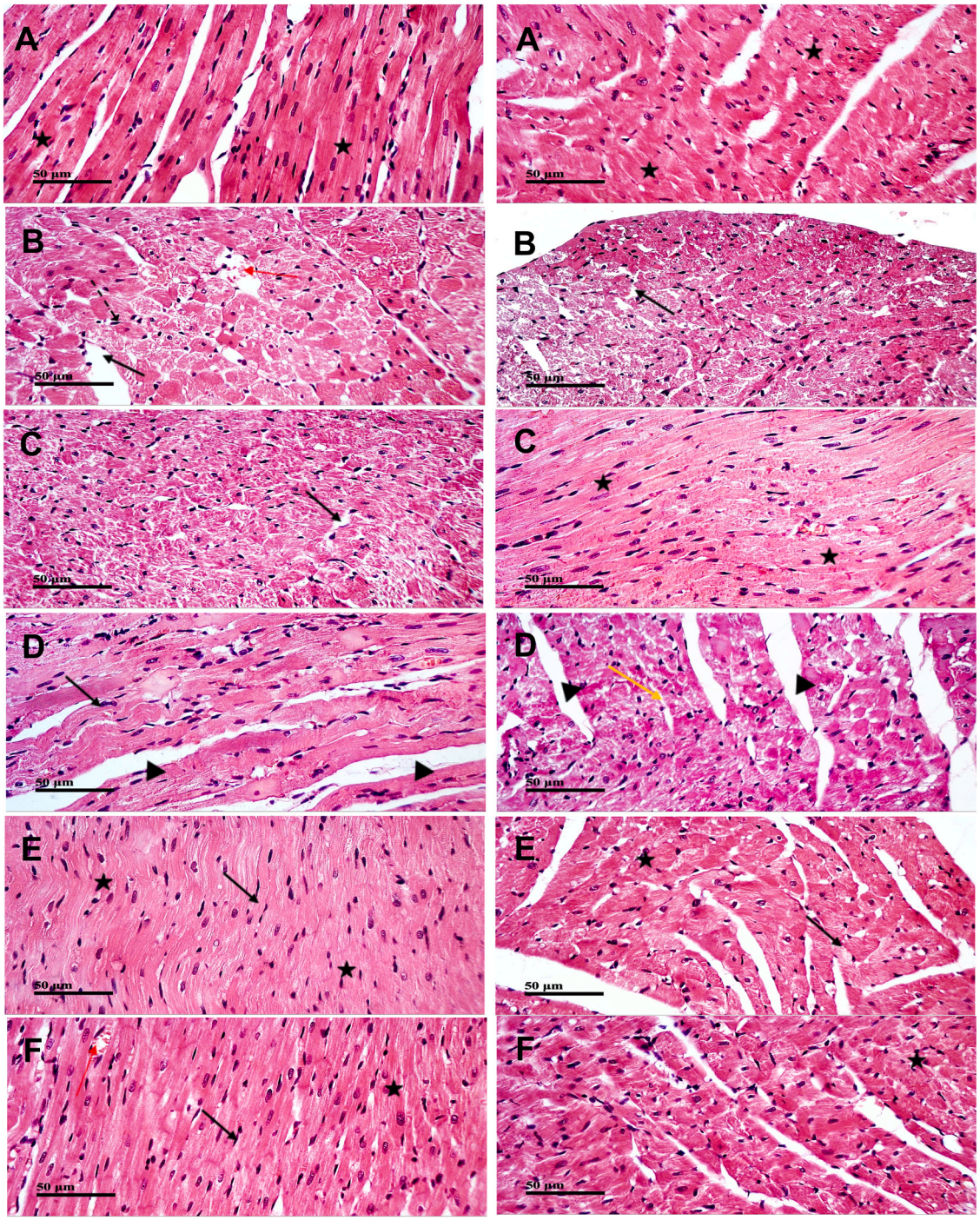

Fig. 3. Effect of NAM or 1α(OH)D_3 on DOX-induced histological alterations of the heart tissue (n = 8–10). (A) Control group: demonstrated normal morphological features of different cardiac wall with apparent intact endocardium, well organized branched striated myocardial muscle fibers *(star)* and delicate epicardium with intact vasculatures, (B) DOX treated group (20 mg/kg) showed focal subendocardial necrosis of cardiomyocytes *(arrow)* with patches of fragmented cardiomyocytes *(arrow)* and degenerated fibers with nuclear pyknosis *(dashed arrow)* accompanied with moderate congestion of intermuscular blood vessels *(red arrow)*, (C) NAM (600 mg/kg) and DOX (20 mg/kg) treated group: showed persistence of alternated apparent intact cardiomyocytes *(star)* and degenerated and fragmented muscle cells *(arrow)* with normal intercellular spaces and minimal inflammatory cells infiltrates, (D) 1α(OH)D_3 (0.5 ug/kg) and DOX (20 mg/kg) treated group showed persistence of wide areas of degenerative changes of cardiomyocytes *(arrow)* with higher intercellular spaces, mild hyalinization *(arrow head)* and few interstitial inflammatory cells infiltrates *(yellow arrow)*., (E) NAM treated group: showed almost intact cardiomyocytes *(star)* and vasculatures with minimal records of degenerative changes *(arrow)* and (F) 1α(OH)D_3 treated group: showed many intact well organized cardiomyocytes with intact vesicular nuclei *(star)* and few records of degenerated cardiac cells *(arrow)* with few congested intermuscular BVs *(red arrow)*.

control group. Interestingly, NAM+DOX-treated group showed a significant reduction in nuclear level of NF-κB by 19% as compared with the DOX group. 1α(OH)D_3 + DOX-treated rats showed a non-significant decrease in the nuclear level of NF-κB when compared with the DOX (Fig. 10H). NAM+DOX-treated rats showed a more significant reduction by 14% over 1α(OH)D_3 + DOX-treated animals.

In linear with NF-κB findings, DOX also provoked a significant rise in IL-6 expression in cardiac tissues by 303% as compared with the control

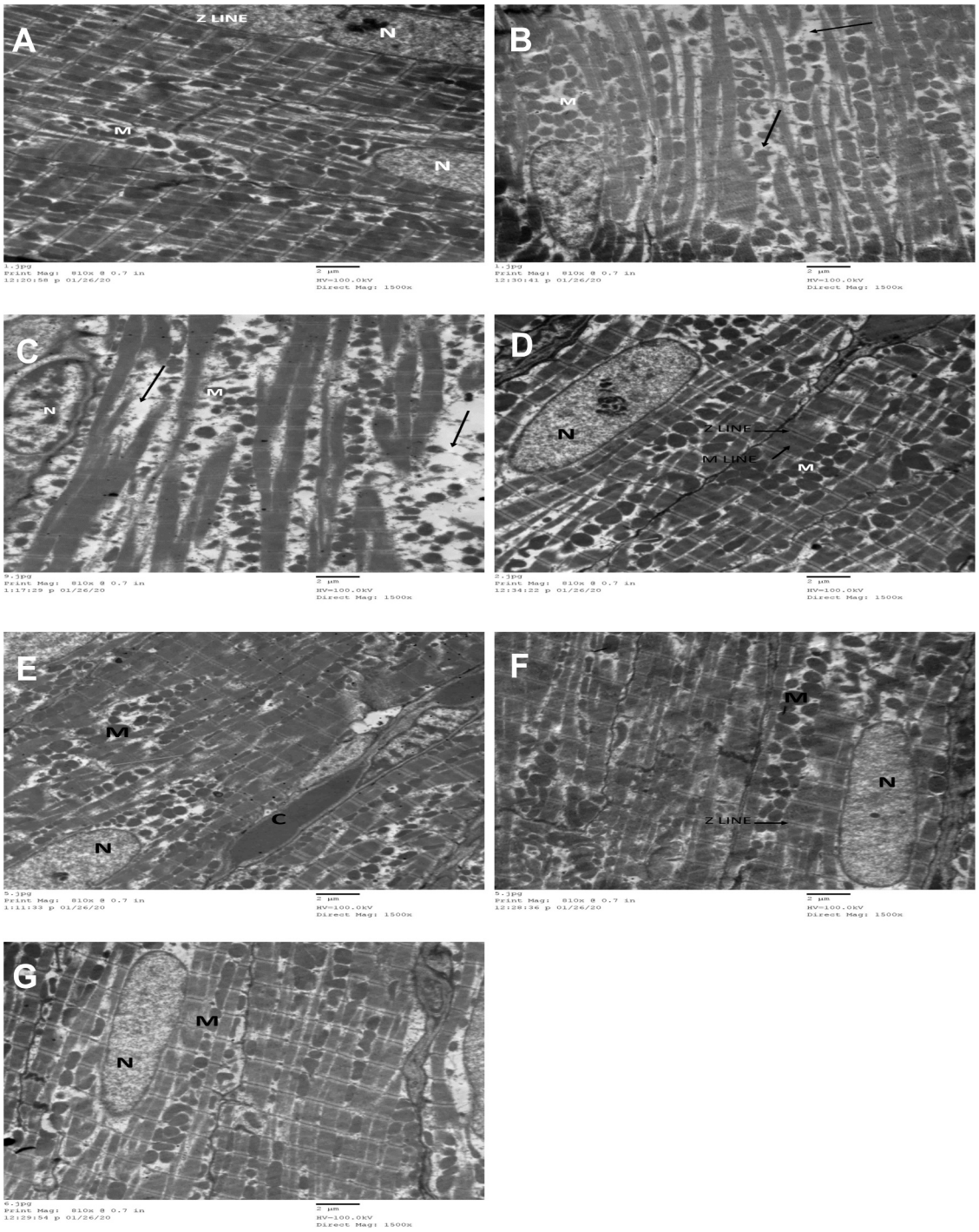

Fig. 4. Electron photomicrographs of NAM or 1α(OH)D_3 on DOX-induced alterations of the heart tissue (n = 8–10). (A) the control group showing that every muscle fiber was a linear unit composed of several cardiac muscle cells joined end to end at specialized junctional zones. Each cell had an elongated nucleus (N) centrally located in the sarcoplasm and was bounded by a sarcolemma. Myofibrils were formed of regular sarcomeres with distinct Z lines. Mitochondria (M) were uniform in size. (B, C) DOX-group showing transmission electron micrographs from a DOX group rats showed B: Electron dense mitochondria (M) of non-uniform size, with loss of inter-mitochondrial contacts and fragmentation. There were areas of myofibril lysis (arrows) with loss of normal sarcomere appearance (B, C). C: Mitochondria were disarranged and non-uniform. (D) NAM and DOX group showing myofibrils formed of regular sarcomeres with distinct Z lines and M lines. Mitochondria (M) were nearly of uniform in size. Minimal areas of myofibril lysis (red arrow). (E) 1α(OH)D_3 and DOX-group showing arranged cardiac muscle fibers, cells joined end to end at specialized junctional zones. Each cell had an elongated nucleus (N) centrally located in the sarcoplasm. Mitochondria (M) were not uniform in size and irregularly arranged. Minimal areas of myofibril lysis (red arrow) area of congestion (C). (F) NAM only: Showed that muscle fiber was a linear unit composed of several cardiac muscle cells joined end to end at specialized junctional zones. Each cell had an elongated nucleus (N) centrally located in the sarcoplasm. Myofibrils are formed of regular arrangement. Mitochondria (M) were uniform in size and arranged between myofibrils. (G) 1α(OH)D_3 only: showed normal architecture.

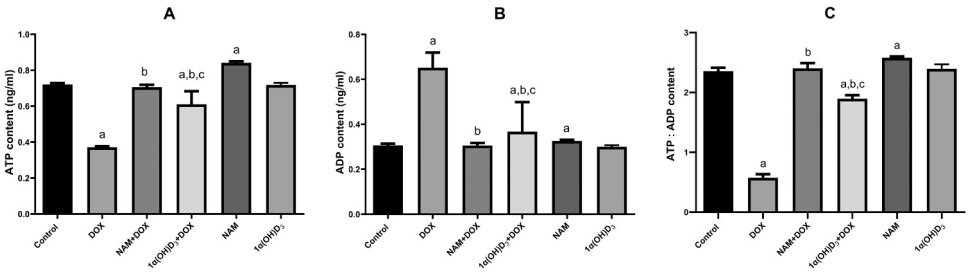

Fig. 5. Effect of NAM or 1α(OH)D_3 on cardiac adenosine triphosphate (ATP), adenosine diphosphate (ADP) and ATP:ADP ratio in DOX-induced cardiotoxicity. (A) shows cardiac ATP content, (B) shows cardiac ADP content, (C) shows cardiac ATP:ADP ratio. Values are means ± SD (n = 8–10). a,b,c: statistically significant from control, DOX or NAM + DOX, respectively at $P < 0.05$ using one-way ANOVA followed by Tukey-Kramer Post Hoc test.

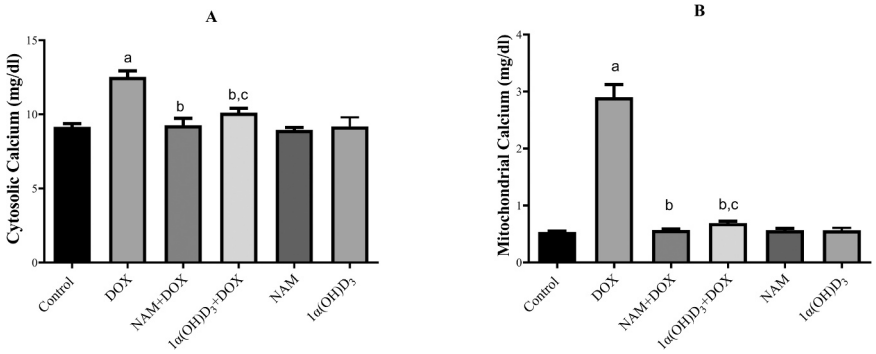

Fig. 6. Effect of NAM or 1α(OH)D_3 on Cytosolic calcium $(Ca^{2+})_i$ and Mitochondrial Calcium $(Ca^{2+})_m$ in cardiac tissue in DOX-induced cardiotoxicity. (A) shows Cytosolic calcium $(Ca^{2+})_i$, (B) shows Mitochondrial Calcium $(Ca^{2+})_m$. Values are means ± SD (n = 8–10). a,b,c: statistically significant from control, DOX or NAM+DOX, respectively at $P < 0.05$ using one-way ANOVA followed by Tukey-Kramer Post Hoc test.

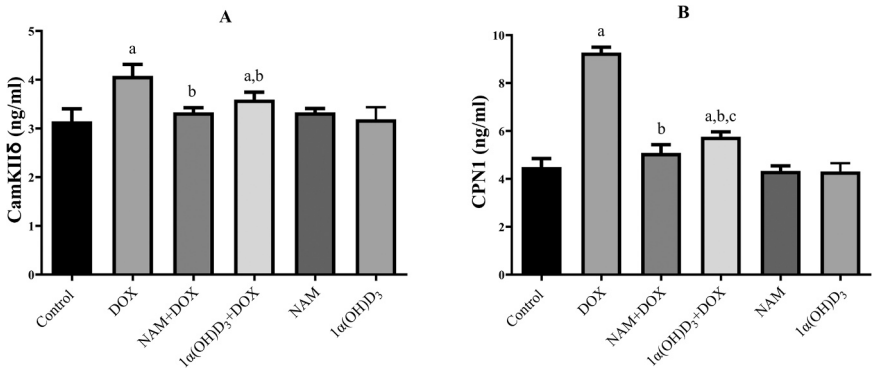

Fig. 7. Effect of NAM or 1α(OH)D_3 on calmodulin kinase II gamma (CAMKIIδ) and calpain (CPN1) in DOX-induced cardiotoxicity. (A) shows CAMKIIδ content in cardiac tissue, (B) shows CPN1 content in cardiac tissue. Values are means ± SD (n = 8–10). a,b,c: statistically significant from control, DOX or NAM+DOX, respectively at $P < 0.05$ using one-way ANOVA followed by Tukey-Kramer Post Hoc test.

group. Conversely, cotreatment of intoxicated animals with either NAM or 1α(OH)D_3 + DOX significantly attenuated the IL-6 levels by 68% and 67%, respectively, compared with the DOX treated group (Fig. 10I). It was obvious that the NAM treated group showed more improvement in NF-κB expression than in the 1α(OH)D_3 treated group. Meanwhile, no significant change was detected in cardiac IL-6 between the two groups.

4. Discussion

Cumulative cardiotoxicity is the most devastating complication associated with DOX therapy [24]. Our aim was to investigate and compare the possible cardioprotective effects of NAM and 1α(OH)D_3 against DOX-induced cardiotoxicity. In this study DOX cardiotoxicity was characterized by conduction abnormalities and a significant elevation in the activities of the serum cardiac enzymes. These biochemical data reflected a severe DOX-induced myocardial injury that was verified by a histopathological examination of cardiac tissues and electron microscopy ultrastructure examination of the cardiac myocytes. On the other hand, DOX affected the mortality of animals by 20%. Nicotinamide (NAM) is the amide form of vitamin B_3 [25]. It is considered as the biosynthetic precursor to nicotinamide adenine dinucleotide (NAD+), nicotinamide adenine dinucleotide phosphate (NADP+) and reduced forms (NAD(P)H) [26]. NAD+ derived cofactors are central to cellular homeostasis as they play a crucial roles in intermediary metabolism, mitochondrial respiration, the Krebs' cycle, ATP production and Ca^{2+} signaling [27]. On the other hand, vitamin D is a steroid hormone derived from cholesterol that is recognized as an important substance for maintaining serum Ca^{2+}homeostasis and bone mineralization [28]. Cellular proliferation, differentiation, reduction of inflammation and immune modulation has been linked to the role of

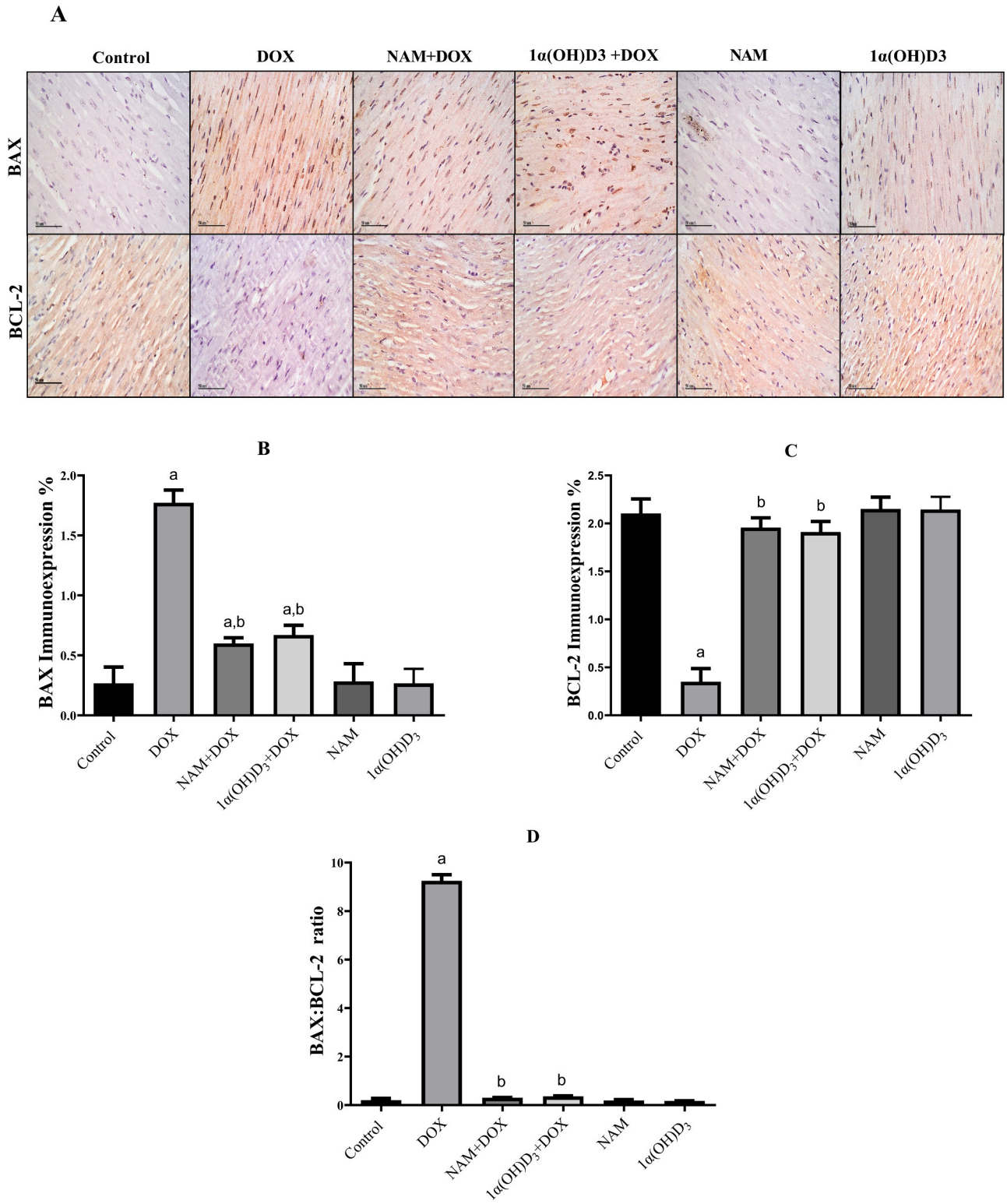

Fig. 8. Effects of NAM or 1α(OH)D_3 on cardiac apoptotic markers (40x) in DOX-induced cardiotoxicity. A: Immunohistochemical staining of cardiac BAX and Bcl-2 expression. B and C: Quantitative image analysis for BAX and Bcl-2 immunohistochemical staining expressed as mean area percent. D: Quantitative image analysis for BAX:Bcl-2 ratio. Data are presented as mean ± SD (n = 8–10). a,b,c: statistically significant from control, DOX, NAM + DOX or 1α(OH)D_3 + DOX, respectively at $P < 0.05$ using one-way ANOVA followed by Tukey-Kramer Post Hoc test.

vitamin D in human body.

Our study showed that NAM and 1α(OH)D_3 significantly preserved cardiac conductivity and biochemical cardiac markers and preserved the normal architecture of cardiomyocytes indicating the promising cardioprotective effects of both NAM and 1α(OH)D_3 against DOX-induced myocardial injury. Our results are consistent with previous studies reporting the promising cardioprotective properties of both vitamins in various experimental models of cardiovascular disorders [20,29,30]. Moreover, both vitamins improved the survival rate of the treated animals.

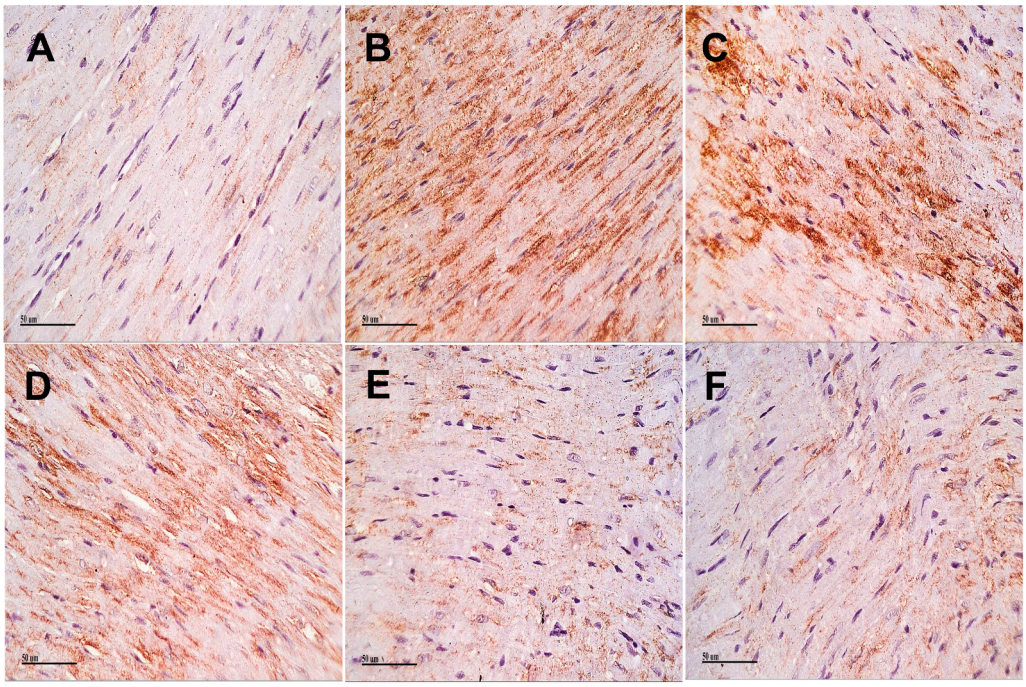

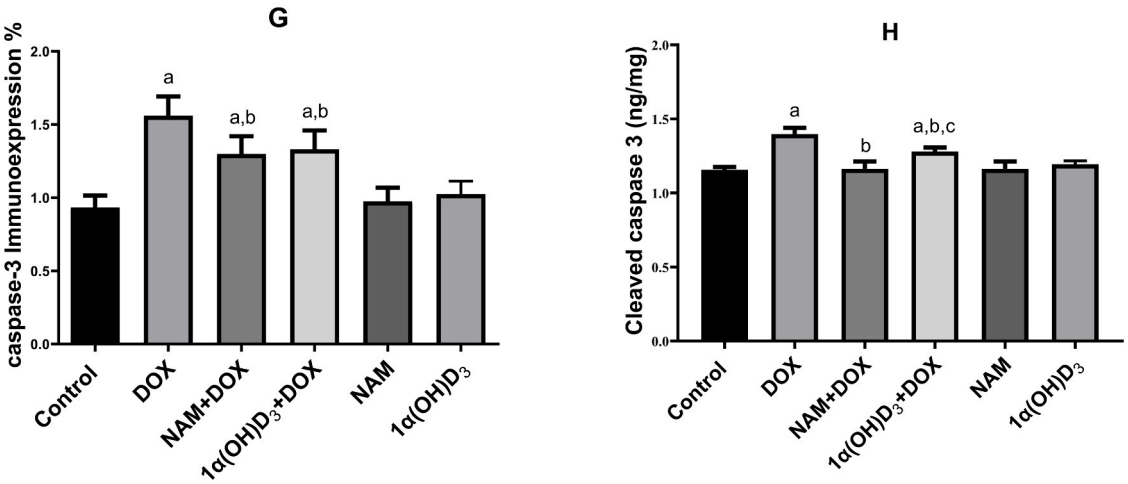

Fig. 9. Effects of NAM or 1α(OH)D_3 on cardiac caspase-3 (40x) and activated caspase-3 (ACASP-3) in DOX-induced cardiotoxicity. A-F: Immunohistochemical staining of cardiac caspase-3 expression. (A) Control group (B) DOX (20 mg/kg) group (C) NAM+DOX treated group (D) 1α(OH)D_3+DOX treated group (E) NAM treated group (F) 1α(OH)D_3 treated group. G: Quantitative image analysis for caspase-3 immunohistochemical staining expressed as mean area percent. Data are presented as mean ± SD (n = 8–10). H: Quantitative analysis for activated caspase-3 in cardiac tissue. Data are presented as mean ± SD (n = 8–10). a,b,c: statistically significant from control, DOX or NAM+DOX, respectively at $P < 0.05$ using one-way ANOVA followed by Tukey-Kramer Post Hoc test.

It should be noted that at the subcellular levels, mitochondria are considered as the primary target for DOX toxic effects [31]. Accumulated DOX in the mitochondria is converted into the unstable semiquinone, which donates electrons to oxygen forming superoxide radicals. Consequently, DOX-driven reactive oxygen species considerably disrupts mitochondrial structure and functionality [32] and hence a depletion of ATP reservoirs and contractile dysfunction of the cardiac muscles [33]. In the current study, DOX-induced impairment in cardiac bioenergetics was reflected by the marked reduction in ATP, elevation in ADP content and decreased ATP:ADP ratio. These findings concur with a previously proven hypothesis that the cardio-selective toxicity of DOX is conferred by the deleterious effects of the drug on mitochondrial bioenergetics [34,35]. In the present study, NAM and 1α(OH)D_3 co-treatments protected the cardiac myocyte bioenergetics as evidenced by preserving ATP generation that was impaired by DOX intoxication. The profound effect of NAM in restoring the ATP generation is probably due to the formation of NAD from its direct precursor NAM, where NAD is immediately metabolized to NAD+ which in turns functions as an electron carrier for ATP generation by mitochondrial respiration [36]. In addition, 1α(OH)D_3 can significantly influence mitochondrial bioenergetics and boost ATP generation by inducing the encoding of several proteins involved in mitochondrial respiratory activity and ATP synthesis [37]. Interestingly, NAM outperformed 1α(OH)D_3 in terms of cardioprotection against DOX-induced cardiac tissue injury in terms of cardiac conductivity, serum cardiac indices and histopathological examination. This could be primarily attributed to increased ATP production to almost normal levels observed with NAM.

One of the notable mechanisms explaining DOX's mitochondrial

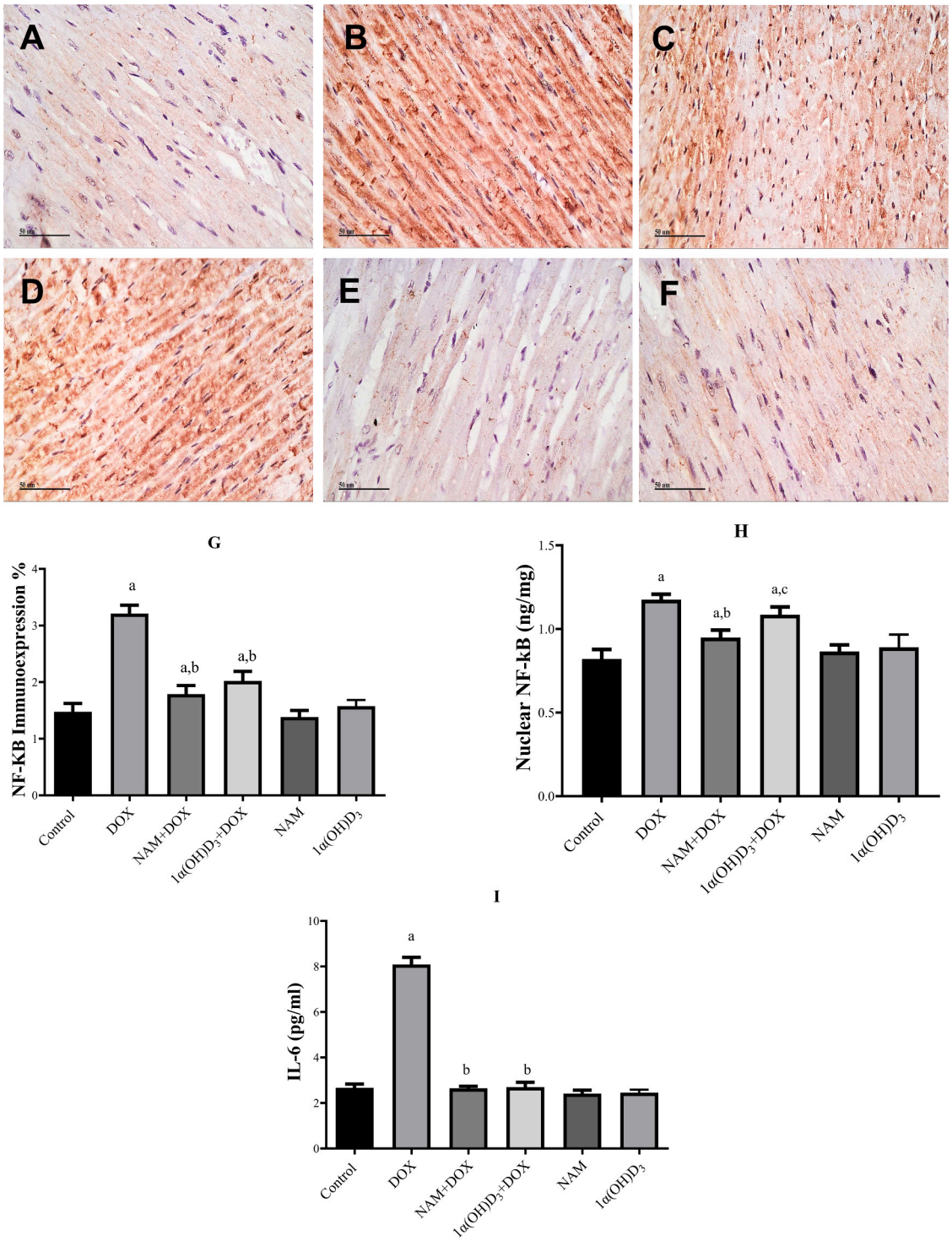

Fig. 10. Effects of NAM or $1\alpha(OH)D_3$ on NF-κB (p65) immunohistochemical expression, nuclear NF-κB and IL-6 level in DOX-induced cardiotoxicity. A-F: Immunohistochemical detection of NF-κB. (A)Control group (B) DOX (20 mg/kg) group (C) NAM+DOX treated group (D) $1\alpha(OH)D_3$+DOX treated group (E) NAM treated group (F) $1\alpha(OH)D_3$ treated group. G: Quantitative image analysis for NF-κB (p65) immunohistochemical staining expressed as mean area percent. Data are presented as mean ± SD (n = 8–10). H: cardiac nuclear NF-κB level. Data are presented as mean ± SD (n = 8–10). I: cardiac IL-6 level. Data are presented as mean ± SD (n = 8–10). a,b,c: statistically significant from control, DOX or NAM+DOX, respectively at $P < 0.05$ using one-way ANOVA followed by Tukey-Kramer Post Hoc test.

damaging effects is dysregulation of intracellular Ca^{2+} homeostasis [30]. DOX is known to affect Ca^{2+} homeostasis by multiple mechanisms including the inhibition of SERCA2a transcription, therefore impeding the Ca^{2+} uptake into sarcoplasmic reticulum (SR) [33]. Moreover, it was reported that DOX can bind to and open the ryanodine receptor (RYR2) thus activating the release of Ca^{2+} from SR into the cytosol [38]. Indeed, in this study both cytosolic and mitochondrial Ca^{2+}were greatly elevated following DOX intoxication. The overload of Ca^{2+} in both cytoplasm and mitochondria were previously reported to be associated with DOX cardiotoxicity [39]. In the current study, the elevated cytosolic and mitochondrial Ca^{2+} concentrations observed in DOX-intoxicated animals were significantly diminished in animals

treated with either NAM or 1α(OH)D_3. By virtue of being vital intermediates in ATP generation, the decrease in Ca^{2+} concentration observed in NAM treated group may be a result of improved SERCA2a pump activity as the SERCA pump is powered by ATP hydrolysis to move Ca^{2+} ions against the concentration gradient to restore cytosolic Ca^{2+} concentration [40]. Similarly, it was reported that NAM could effectively foster the activity of SERCA2a pump and preserve Ca^{2+} homeostasis that account for its neuroprotective effects in spinocerebellar ataxia [41]. While reports on the role of 1α(OH)D_3 in regulating intracellular Ca^{2+} levels are controversial, several studies have indicated that vitamin D deficiency is associated with intracellular Ca^{2+} overload, which contributes to neuronal cell death and dementia [42]. The current findings coincided also with another study demonstrating repressed SERCA pump expression and abnormal Ca^{2+} handling in case of defective vitamin D signaling resulting in exaggerated cardiac dysfunction in mice [43].

The activation of many Ca^{2+} based cysteine proteases is linked to intracellular Ca^{2+} overload. Calpains, which play important roles in the execution of apoptosis, are one of these important proteases [34]. Once activated, CPN1 provokes proteolysis of numerous membrane, cytoplasmic and nuclear proteins, resulting in degradation of cellular architecture and finally apoptosis [44]. In the current study, DOX prompted a significant rise in CPN1 expression in cardiac myocytes. This finding is in agreement with a previous study confirming the role of Ca^{2+} dependent, CPN1-mediated apoptotic pathways in DOX-induced myocardial injury [45]. The present study showed that NAM and 1α(OH)D_3 significantly inhibited cardiac CPN1 expression in DOX intoxicated animals. To the best of our knowledge, this is the first study to report that the anti-apoptotic effects of both vitamins are linked to their abilities to downgrade expression of the CPN1 enzyme in cardiac tissue. Furthermore, our study showed that NAM exhibited greater anti-apoptotic effects than those of 1α(OH)D_3.

On the other hand, mitochondrial Ca^{2+} overload is critical in initiating the intrinsic apoptotic pathway where it induces permeabilization of mitochondrial outer membrane and in turn the release of mitochondrial apoptotic factors such as cytochrome c into the cytosol [46] which then prompts the activation of initiator caspase-9 which further activates the executer caspase-3 [47]. In this regard, the permeability of the mitochondrial membrane is tightly regulated by a family of proteins called the Bcl-2 family. This family encompasses pro-apoptotic members such as Bax and anti-apoptotic members such as Bcl-2 [48]. In the current work, DOX intoxication switched on the mitochondrial-dependent apoptotic machinery through upregulating Bax protein, and downregulating Bcl-2 protein hence inducing the expression of caspase-3 enzyme. These findings are in accordance with several studies proving the role of the intrinsic apoptotic pathway in the pathogenesis of DOX cardiotoxicity [19,49]. In this regard, the current study has ascertained potent antiapoptotic properties of both NAM and 1α(OH)D_3 as a chief mechanism for their cardioprotective capabilities as evidenced by downregulating of the apoptotic markers; Bax and caspase 3 enzyme while upregulating the antiapoptotic marker; Bcl-2. The findings are in accordance with previous studies which advocated that the cytoprotective properties of both vitamins were primarily due to their abilities to repress the intrinsic apoptotic cascades through modulating expression of Bcl-2 family proteins thus maintaining mitochondrial membrane integrity [50,51].

In addition to the key role of the apoptotic pathway, exaggerated inflammatory responses play vital roles in the pathogenesis of DOX-induced cardiomyopathy [52]. Increasing evidences indicate that DOX-induced inflammation is attributed mainly to the upregulation of the transcription factor NF-κB [53]. NF-κB is a corner stone in the regulation of inflammatory responses. NF-κB complex exists in an inactive state in the cytoplasm. Upon stimulation by various inducers, the ultimate NF-κB dimer translocates to the nucleus, where it binds to the responsive DNA sequences and upregulates the expression of numerous inflammatory cytokines such as IL-6 [54]. Notably, in the current study DOX-induced cardiotoxicity is associated with amplified proinflammatory responses as shown by upregulating inflammatory mediators; NF-κB and IL-6 which came along with previous studies that proved that triggering inflammatory cascades is an integral player in the pathogenesis of DOX-induced cardiomyopathy [55,56].

Our results reported the powerful anti-inflammatory properties of both NAM and 1α(OH)D_3 as another key mechanism underlying the promising cardioprotective effects of both vitamins against DOX-induced cardiotoxicity as shown by downregulating both the inflammatory markers; NF-κB and IL-6. In accordance with our study, NAM effectively demonstrated anti-inflammatory properties in various experimental models such as LPS-induced septic shock mainly through suppressing the expression of pro-inflammatory cytokines and downregulating NF-κB activation [57]. Besides, vitamin D supplementation effectively halts the progression of coronary artery diseases by repressing nuclear translocation of freely available cytoplasmic NF-κB complexes thus decreasing the expression of subsequent pro-inflammatory genes [58].

The Ca^{2+} calmodulin-dependent protein kinases are crucial transducers of Ca^{2+} signals thus controlling a network of Ca^{2+}-dependent biochemical processes [59]. The Ca^{2+}/calmodulin-dependent protein kinase II-gamma (CaMKIIδ), the predominant isoform in the heart, is a multifunctional serine/threonine-specific protein kinase that plays a pivotal role in the regulation of a diverse array of cellular processes including cardiomyocyte Ca^{2+} cycling, contractility, inflammation and cell survival via the phosphorylation of a multitude of downstream targets [60,61]. CaMKIIδ contributes in modulating cardiac myocyte Ca^{2+} handling by phosphorylating several Ca^{2+} regulating proteins including RyR2. Phosphorylated RyR2 induce SR Ca^{2+} leakage into the cytosol leading to cellular Ca^{2+}overload, thereby impairing cardiac contractility [62]. Additionally, CaMKIIδ activation can trigger cardiomyocyte death by promoting Ca^{2+} flux from SR to the mitochondria resulting in mitochondrial permeability transition and consequently switching on the intrinsic apoptotic machinery [63–65]. Furthermore, it has been recently reported that CaMKIIδ can promote myocardial ischemia/reperfusion injury by activating the Ca^{2+} regulated protease; calpain [66].

Moreover, CaMKIIδ plays a role in regulation of the immune and inflammatory responses by provoking phosphorylation and activation of the IKK complex hence activating the transcriptional activity of NF-κB and the subsequent production of inflammatory genes production [67]. Indeed, in the current study DOX intoxication upregulated NF-κB activity. These findings were consistent with previous ones revealing the fundamental role of CaMKIIδ in DOX-induced cardiomyopathy [6,68]. Interestingly, both NAM & 1α(OH)D_3 significantly reduced CaMKIIδ activity. In agreement with our findings, it was reported that CaMKIIδ activation is induced by defective vitamin D signaling [69]. In addition, NAD depletion is found to be associated with elevated CaMKIIδ activity [70]. Curiously, NAM showed a better Ca^{2+} homeostasis effect compared with 1α(OH)D_3, that may be attributed to its ability to maintain adequate ATP required for the active Ca^{2+} channels to preserve Ca^{2+} levels to normal.

In conclusion, the current study proved the promising cardioprotective effects of NAM and 1α(OH)D_3 against DOX-induced cardiomyopathy. Both NAM and 1α(OH)D_3 ameliorated the cardiotoxic effects of DOX. Moreover, the study has uncovered various molecular mechanisms responsible for these cardioprotective properties in the term of replenishing ATP stores, preserving intracellular and mitochondrial Ca^{2+} homeostasis, suppressing mitochondrial and CPN1-mediated apoptotic cascades and abrogating NF-κB - triggered inflammatory responses. Moreover, a novel finding of this study was exploring the inhibitory effect of both NAM and 1α(OH)D_3 on the pivotal Ca^{2+} transducer CaMKIIδ which is extensively implicated in DOX-induced Ca^{2+} overload, inflammatory and apoptotic signals. Furthermore, our study clarifies that, NAM has a superior cardioprotective effect over 1α(OH)D_3, with regard to increasing ATP production, reducing both

mitochondrial and cytosolic Ca^{2+} and downregulation of CaMKIIδ, CPN1 and inflammatory markers. These findings advocate the pharmacological benefits of both nutraceuticals as adjunctive therapy with DOX for halting the progression of its associated devastating cardiac complications. Future mechanistic and clinical studies are warranted to support our findings.

Funding

This research did not receive any specific grant from funding agencies in the public, commercial, or not-for-profit sectors.

Conflict of interest statement

The author has read the journal's policy on disclosure of potential conflicts of interest and declared no personal or financial conflict of interest.

References

[1] B.A and K.S. Wakharde AA, Awad AH, Synergistic Activation of Doxorubicin Against Cancer: A Review, 1009, 2018.
[2] L. Xi, S.G. Zhu, A. Das, Q. Chen, D. Durrant, D.C. Hobbs, E.J. Lesnefsky, R. C. Kukreja, Dietary inorganic nitrate alleviates doxorubicin cardiotoxicity: mechanisms and implications, Nitric Oxide Biol. Chem. 26 (2012) 274–284, https://doi.org/10.1016/j.niox.2012.03.006.
[3] A. Pugazhendhi, T.N.J.I. Edison, B.K. Velmurugan, J.A. Jacob, I. Karuppusamy, Toxicity of doxorubicin (Dox) to different experimental organ systems, Life Sci. 200 (2018) 26–30, https://doi.org/10.1016/j.lfs.2018.03.023.
[4] S. Zhou, L.J. Heller, K.B. Wallace, Interference with calcium-dependent mitochondrial bioenergetics in cardiac myocytes isolated from doxorubicin-treated rats, Toxicol. Appl. Pharmacol. 175 (2001) 60–67.
[5] Y.M. Jang, S. Kendaiah, B. Drew, T. Phillips, C. Selman, D. Julian, C. Leeuwenburgh, Doxorubicin treatment in vivo activates caspase-12 mediated cardiac apoptosis in both male and female rats, FEBS Lett. 577 (2004) 483–490, https://doi.org/10.1016/j.febslet.2004.10.053.
[6] H. Tscheschner, E. Meinhardt, P. Schlegel, A. Jungmann, L.H. Lehmann, O. J. Müller, P. Most, H.A. Katus, P.W. Raake, CaMKII activation participates in doxorubicin cardiotoxicity and is attenuated by moderate GRP78 overexpression, PLoS One 14 (2019), 0215992, https://doi.org/10.1371/journal.pone.0215992.
[7] L.-H. Kong, X.-M. Gu, F. Wu, Z.-X. Jin, J.-J. Zhou, CaMKII inhibition mitigates ischemia/reperfusion-elicited calpain activation and the damage to membrane skeleton proteins in isolated rat hearts, Biochem. Biophys. Res. Commun. 491 (2017) 687–692.
[8] P. Pasdois, J.E. Parker, A.P. Halestrap, Extent of mitochondrial hexokinase II dissociation during ischemia correlates with mitochondrial cytochrome c release, reactive oxygen species production, and infarct size on reperfusion, JAHA 2 (2013), e005645, https://doi.org/10.1161/JAHA.112.005645.
[9] R.A. Shaker, S.H. Abboud, H.C. Assad, N. Hadi, Enoxaparin attenuates doxorubicin induced cardiotoxicity in rats via interfering with oxidative stress, inflammation and apoptosis, BMC Pharmacol. Toxicol. 19 (2018) 1–10, https://doi.org/10.1186/s40360-017-0184-z.
[10] B. Kalyanaraman, Teaching the basics of the mechanism of doxorubicin-induced cardiotoxicity: Have we been barking up the wrong tree? Redox Biol. 29 (2020), 101394 https://doi.org/10.1016/j.redox.2019.101394.
[11] V. Lobo, A. Patil, A. Phatak, N. Chandra, Free radicals, antioxidants and functional foods: impact on human health, Pharmacogn. Rev. 4 (2010) 118–126, https://doi.org/10.4103/0973-7847.70902.
[12] N. Wolak, M. Zawrotniak, M. Gogol, A. Kozik, M. Rapala-Kozik, Vitamins B1, B2, B3 and B9 – occurrence, biosynthesis pathways and functions in human nutrition, mini-reviews, Med. Chem. 17 (2016) 1075–1111, https://doi.org/10.2174/1389557516666160725095729.
[13] L.J. Hill, A.C. Williams, Meat Intake and the Dose of Vitamin B3-Nicotinamide, 2017.
[14] K.A. Hershberger, A.S. Martin, M.D. Hirschey, Role of NAD+ and mitochondrial sirtuins in cardiac and renal diseases, Nat. Rev. Nephrol. 13 (2017) 213–225, https://doi.org/10.1038/nrneph.2017.5.
[15] S.J. Wimalawansa, Vitamin D deficiency: effects on oxidative stress, epigenetics, gene regulation, and aging, Biology 8 (2019) 30, https://doi.org/10.3390/biology8020030.
[16] F. Saponaro, C. Marcocci, R. Zucchi, C. Prontera, A. Clerico, M. Scalese, S. Frascarelli, A. Saba, C. Passino, Hypovitaminosis D in patients with heart failure: effects on functional capacity and patients' survival, Endocrine 58 (2017) 574–581, https://doi.org/10.1007/s12020-017-1282-9.
[17] S. Cruciani, S. Santaniello, G. Garroni, A. Fadda, F. Balzano, E. Bellu, G. Sarais, G. Fais, M. Mulas, M. Maioli, Myrtus polyphenols, from antioxidants to anti-inflammatory molecules: exploring a network involving cytochromes P450 and Vitamin D, Molecules 24 (2019) 1515, https://doi.org/10.3390/molecules24081515.
[18] R. Wei, S. Christakos, Mechanisms underlying the regulation of innate and adaptive immunity by vitamin D, Nutrients 7 (2015) 8251–8260, https://doi.org/10.3390/nu7105392.
[19] E.M. Mantawy, A. Esmat, W.M. El-Bakly, R.A. Salah Eldin, E. El-Demerdash, Mechanistic clues to the protective effect of chrysin against doxorubicin-induced cardiomyopathy: plausible roles of p53, MAPK and AKT pathways, Sci. Rep. 7 (2017) 1–13, https://doi.org/10.1038/s41598-017-05005-9.
[20] O.A. El-Gohary, M.M. Allam, Effect of vitamin D on isoprenaline-induced myocardial infarction in rats: possible role of peroxisome proliferator-activated receptor-γ, Can. J. Physiol. Pharmacol. 95 (2017) 641–646, https://doi.org/10.1139/cjpp-2016-0150.
[21] J.J. Bozzola, L.D. Russell, Electron biology principles and techniques for biologists, Jones Bartlett Learn. (1999).
[22] D. Johnson, H. Lardy, Isolation of liver or kidney mitochondria, in: Methods Enzymol, Elsevier, 1967, pp. 94–96, https://doi.org/10.1016/0076-6879(67)10018-9.
[23] H. Gitelman, An improved automated procedure for the determination of calcium in biological specimens, Anal. Biochem. 18 (1967) 521–531.
[24] T.R. Mancilla, B. Iskra, G.J. %J C.P. Aune, doxorubicin-induced cardiomyopathy in, Children 9 (2011) 905–931.
[25] R.A. Fricker, E.L. Green, S.I. Jenkins, S.M. Griffin, The influence of nicotinamide on health and disease in the central nervous system, 1178646918776658, Int. J. Tryptophan Res. 11 (2018), 1178646918776658, https://doi.org/10.1177/1178646918776658.
[26] M.V. Makarov, S.A.J. Trammell, M.E. Migaud, The chemistry of the vitamin B3 metabolome, Biochem. Soc. Trans. 47 (2019) 131–147.
[27] E. Verdin, NAD+ in aging, metabolism, and neurodegeneration, Science 350 (2015) 1208–1213, https://doi.org/10.1126/science.aac4854.
[28] D. Vitamin, Fact sheet for health professionals, Natl. Institutes Health Off. Diet. Suppl. Website. 2017.
[29] A.M. Abood, M.F. Elshal, VDR stimulation improves outcome of isoprenaline-induced myocardial infarction in rats via down-regulation of cardiac inos gene expression, Biomed. Res. 26 (2015) 755–764.
[30] N. Wenningmann, M. Knapp, A. Ande, T.R. Vaidya, S. Ait-Oudhia, Insights into doxorubicin-induced cardiotoxicity: molecular mechanisms, preventive strategies, and early monitoring, Mol. Pharmacol. 96 (2019) 219–232, https://doi.org/10.1124/mol.119.115725.
[31] J. Yin, J. Guo, Q. Zhang, L. Cui, L. Zhang, T. Zhang, J. Zhao, J. Li, A. Middleton, P. L. Carmichael, Doxorubicin-induced mitophagy and mitochondrial damage is associated with dysregulation of the PINK1/parkin pathway, Toxicol. Vitr. 51 (2018) 1–10.
[32] K. Min, O.S. Kwon, A.J. Smuder, M.P. Wiggs, K.J. Sollanek, D.D. Christou, J.K. Yoo, M.H. Hwang, H.H. Szeto, A.N. Kavazis, S.K. Powers, Increased mitochondrial emission of reactive oxygen species and calpain activation are required for doxorubicin-induced cardiac and skeletal muscle myopathy, J. Physiol. 593 (2015) 2017–2036, https://doi.org/10.1113/jphysiol.2014.286518.
[33] S. Gorini, A. De Angelis, L. Berrino, N. Malara, G. Rosano, E. Ferraro, Chemotherapeutic drugs and mitochondrial dysfunction: focus on doxorubicin, trastuzumab, and sunitinib, Oxid. Med. Cell. Longev. 2018 (2018), 7582730, https://doi.org/10.1155/2018/7582730.
[34] R. Wu, P.A. Yao, H.L. Wang, Y. Gao, H.L. Yu, L. Wang, X.H. Cui, X. Xu, J.P. Gao, Effect of fermented cordyceps sinensis on doxorubicin-induced cardiotoxicity in rats, Mol. Med. Rep. 18 (2018) 3229–3241, https://doi.org/10.3892/mmr.2018.9310.
[35] R. Wu, H.L. Wang, H.L. Yu, X.H. Cui, M.T. Xu, X. Xu, J.P. Gao, Doxorubicin toxicity changes myocardial energy metabolism in rats, Chem. Biol. Interact. 244 (2016) 149–158, https://doi.org/10.1016/j.cbi.2015.12.010.
[36] N. Xie, L. Zhang, W. Gao, C. Huang, P.E. Huber, X. Zhou, C. Li, G. Shen, B. Zou, NAD+ metabolism: pathophysiologic mechanisms and therapeutic potential, Signal Transduct. Target. Ther. 5 (2020) 1–37.
[37] Z.C. Ryan, T.A. Craig, C.D. Folmes, X. Wang, I.R. Lanza, N.S. Schaible, J. L. Salisbury, K.S. Nair, A. Terzic, G.C. Sieck, R. Kumar, 1α,25-dihydroxyvitamin D3 regulates mitochondrial oxygen consumption and dynamics in human skeletal muscle cells, J. Biol. Chem. 291 (2016) 1514–1528, https://doi.org/10.1074/jbc.M115.684399.
[38] S. Upadhyay, K.B. Gupta, A.K. Mantha, M. Dhiman, A short review: doxorubicin and its effect on cardiac proteins, J. Cell. Biochem. 122 (2021) 153–165.
[39] F.D. Agustini, W. Arozal, M. Louisa, S. Siswanto, V. Soetikno, N. Nafrialdi, F. Suyatna, Cardioprotection mechanism of mangiferin on doxorubicin-induced rats: focus on intracellular calcium regulation, Pharm. Biol. 54 (2016) 1289–1297, https://doi.org/10.3109/13880209.2015.1073750.
[40] M. Periasamy, A. Kalyanasundaram, SERCA pump isoforms: their role in calcium transport and disease, Muscle Nerve 35 (2007) 430–442, https://doi.org/10.1002/mus.20745.
[41] C.A. Stoyas, D.D. Bushart, P.M. Switonski, J.M. Ward, A. Alaghatta, M. bo Tang, C. Niu, M. Wadhwa, H. Huang, A. Savchenko, K. Gariani, F. Xie, J.R. Delaney, T. Gaasterland, J. Auwerx, V.G. Shakkottai, A.R. La Spada, Nicotinamide pathway-dependent sirt1 activation restores calcium homeostasis to achieve neuroprotection in spinocerebellar ataxia type 7, Neuron 105 (2020) 630–644.e9, https://doi.org/10.1016/j.neuron.2019.11.019.
[42] M.J. Berridge, Vitamin D, reactive oxygen species and calcium signalling in ageing and disease, Philos. Trans. R. Soc. Lond. B Biol. Sci. 371 (2016), 20150434, https://doi.org/10.1098/rstb.2015.0434.
[43] S. Choudhury, S. Bae, Q. Ke, J.Y. Lee, S.S. Singh, R. St-Arnaud, F. Del Monte, P. M. Kang, Abnormal calcium handling and exaggerated cardiac dysfunction in mice

with defective vitamin d signaling, PLoS One 9 (2014), 108382, https://doi.org/10.1371/journal.pone.0108382.
[44] X. Teng, C. Ji, H. Zhong, D. Zheng, R. Ni, D.J. Hill, S. Xiong, G.C. Fan, P.A. Greer, Z. Shen, T. Peng, Selective deletion of endothelial cell calpain in mice reduces diabetic cardiomyopathy by improving angiogenesis, Diabetologia 62 (2019) 860–872, https://doi.org/10.1007/s00125-019-4828-y.
[45] D. Zheng, Z. Su, Y. Zhang, R. Ni, G.C. Fan, J. Robbins, L.S. Song, J. Li, T. Peng, Calpain-2 promotes MKP-1 expression protecting cardiomyocytes in both in vitro and in vivo mouse models of doxorubicin-induced cardiotoxicity, Arch. Toxicol. 93 (2019) 1051–1065, https://doi.org/10.1007/s00204-019-02405-w.
[46] S.H. Suhaili, H. Karimian, M. Stellato, T.H. Lee, M.I. Aguilar, Mitochondrial outer membrane permeabilization: a focus on the role of mitochondrial membrane structural organization, Biophys. Rev. 9 (2017) 443–457, https://doi.org/10.1007/s12551-017-0308-0.
[47] S. Elmore, Apoptosis: a review of programmed cell death, Toxicol. Pathol. 35 (2007) 495–516, https://doi.org/10.1080/01926230701320337.
[48] F. Edlich, BCL-2 proteins and apoptosis: recent insights and unknowns, Biochem. Biophys. Res. Commun. 500 (2018) 26–34, https://doi.org/10.1016/j.bbrc.2017.06.190.
[49] U. Michihiko, K. Yoshihiko, Y. Koh-ichi, M. Nobuyuki, I. Motoyuki, M. Takashi, Y. Iwao, Doxorubicin induces apoptosis by activation of caspase-3 in cultured cardiomyocytes in vitro and rat cardiac ventricles in vivo, J. Pharmacol. Sci. 101 (2006) 151–158.
[50] Y.F. Lai, L. Wang, W.Y. Liu, Nicotinamide pretreatment alleviates mitochondrial stress and protects hypoxic myocardial cells via AMPK pathway, Eur. Rev. Med. Pharmacol. Sci. 23 (2019) 1797–1806, https://doi.org/10.26355/eurrev_201902_17143.
[51] X. Guo, H. Lin, J. Liu, D. Wang, D. Li, C. Jiang, Y. Tang, J. Wang, T. Zhang, Y. Li, P. Yao, 1,25-Dihydroxyvitamin D attenuates diabetic cardiac autophagy and damage by vitamin D receptor-mediated suppression of FoxO1 translocation, J. Nutr. Biochem. 80 (2020), 108380, https://doi.org/10.1016/j.jnutbio.2020.108380.
[52] L. Guo, X. Zheng, E. Wang, X. Jia, G. Wang, J. Wen, Irigenin treatment alleviates doxorubicin (DOX)-induced cardiotoxicity by suppressing apoptosis, inflammation and oxidative stress via the increase of miR-425, Biomed. Pharmacother. 125 (2020), 109784.
[53] Q.L. Zhang, J.J. Yang, H.S. Zhang, Carvedilol (CAR) combined with carnosic acid (CAA) attenuates doxorubicin-induced cardiotoxicity by suppressing excessive oxidative stress, inflammation, apoptosis and autophagy, Biomed. Pharmacother. 109 (2019) 71–83, https://doi.org/10.1016/j.biopha.2018.07.037.
[54] B.C. Albensi, What is nuclear factor kappa B (NF-κB) doing in and to the mitochondrion? Front. Cell Dev. Biol. 7 (2019) 154, https://doi.org/10.3389/fcell.2019.00154.
[55] S. Ikeda, S. Matsushima, K. Okabe, M. Ikeda, A. Ishikita, T. Tadokoro, N. Enzan, T. Yamamoto, M. Sada, H. Deguchi, S. Morimoto, T. Ide, H. Tsutsui, Blockade of L-type Ca2+ channel attenuates doxorubicin-induced cardiomyopathy via suppression of CaMKII-NF-κB pathway, Sci. Rep. 9 (2019) 1–14, https://doi.org/10.1038/s41598-019-46367-6.
[56] M. Narikawa, M. Umemura, R. Tanaka, M. Hikichi, A. Nagasako, T. Fujita, U. Yokoyama, T. Ishigami, K. Kimura, K. Tamura, Y. Ishikawa, Doxorubicin induces trans-differentiation and MMP1 expression in cardiac fibroblasts via cell death-independent pathways, PLoS One 14 (2019), 0221940, https://doi.org/10.1371/journal.pone.0221940.
[57] J.S. Ungerstedt, M. Blombäck, T. Söderström, Nicotinamide is a potent inhibitor of proinflammatory cytokines, Clin. Exp. Immunol. 131 (2003) 48–52, https://doi.org/10.1046/j.1365-2249.2003.02031.x.
[58] S. Chen, V.J. Swier, C.S. Boosani, M.M. Radwan, D.K. %J A. Agrawal thrombosis, V. Biology, Vitamin D deficiency accelerates coronary artery disease progression in swine, Arterioscler. Thromb. Vasc. Biol. 36 (2016) 1651–1659, https://doi.org/10.1161/ATVBAHA.116.307586.
[59] S.K. Mohankumar, C.G. Taylor, P. Zahradka, Domain-dependent modulation of insulin-induced AS160 phosphorylation and glucose uptake by Ca 2+/calmodulin-dependent protein kinase II in L6 myotubes, Cell. Signal. 24 (2012) 302–308, https://doi.org/10.1016/j.cellsig.2011.09.014.
[60] J.R. Erickson, Mechanisms of CaMKII activation in the heart, Front. Pharmacol. 5 (2014) 59, https://doi.org/10.3389/fphar.2014.00059.
[61] M.E. Anderson, Oxidant stress promotes disease by activating CaMKII, J. Mol. Cell. Cardiol. 89 (2015) 160–167, https://doi.org/10.1016/j.yjmcc.2015.10.014.
[62] S.O. Marx, A.R. Marks, Dysfunctional ryanodine receptors in the heart: new insights into complex cardiovascular diseases, J. Mol. Cell. Cardiol. 58 (2013) 225–231, https://doi.org/10.1016/j.yjmcc.2013.03.005.
[63] M. Sepúlveda, L.A. Gonano, M. Viotti, M. Morell, P. Blanco, M. López Alarcón, I. Peroba Ramos, A. Bastos Carvalho, E. Medei, M. Vila Petroff, Calcium/calmodulin protein kinase II-dependent ryanodine receptor phosphorylation mediates cardiac contractile dysfunction associated with sepsis, Crit. Care Med. 45 (2017) e399–e408, https://doi.org/10.1097/CCM.0000000000002101.
[64] H. Uchinoumi, Y. Yang, T. Oda, N. Li, K.M. Alsina, J.L. Puglisi, Y. Chen-Izu, R. L. Cornea, X.H.T. Wehrens, D.M. Bers, CaMKII-dependent phosphorylation of RyR2 promotes targetable pathological RyR2 conformational shift, J. Mol. Cell. Cardiol. 98 (2016) 62–72, https://doi.org/10.1016/j.yjmcc.2016.06.007.
[65] M.H. Olofsson, A.M. Havelka, S. Brnjic, M.C. Shoshan, S. Linder, Charting calcium-regulated apoptosis pathways using chemical biology: Role of calmodulin kinase II, BMC Chem. Biol. 8 (2008) 2, https://doi.org/10.1186/1472-6769-8-2.
[66] H.T. Lu, R.Q. Feng, J.K. Tang, J.J. Zhou, F. Gao, J. Ren, CaMKII/calpain interaction mediates ischemia/reperfusion injury in isolated rat hearts, Cell Death Dis. 11 (2020) 1–13, https://doi.org/10.1038/s41419-020-2605-y.
[67] G. Maubach, O. Sokolova, M. Wolfien, H.J. Rothkötter, M. Naumann, Ca2+/calmodulin-dependent kinase II contributes to inhibitor of nuclear factor-kappa B kinase complex activation in Helicobacter pylori infection, Int. J. Cancer 133 (2013) 1507–1512, https://doi.org/10.1002/ijc.28148.
[68] C.M. Sag, A.C. Köhler, M.E. Anderson, J. Backs, L.S. Maier, CaMKII-dependent SR Ca leak contributes to doxorubicin-induced impaired Ca handling in isolated cardiac myocytes, J. Mol. Cell. Cardiol. 51 (2011) 749–759, https://doi.org/10.1016/j.yjmcc.2011.07.016.
[69] J. Oh, A.E. Riek, I. Darwech, K. Funai, J.S. Shao, K. Chin, O.L. Sierra, G. Carmeliet, R.E. Ostlund, C. Bernal-Mizrachi, Deletion of macrophage vitamin D receptor promotes insulin resistance and monocyte cholesterol transport to accelerate atherosclerosis in mice, Cell Rep. 10 (2015) 1872–1886, https://doi.org/10.1016/j.celrep.2015.02.043.
[70] M. Takeuchi, T. Yamamoto, Apoptosis induced by NAD depletion is inhibited by KN-93 in a CaMKII-independent manner, Exp. Cell Res. 335 (2015) 62–67, https://doi.org/10.1016/j.yexcr.2015.05.019.